Journal of Microbiology (2017) Vol. 55, No. 10, pp. 783–791
DOI 10.1007/s12275-017-7259-9
eISSN 1976-3794
pISSN 1225-8873

Silencing the cleavage factor CFIm25 as a new strategy to control *Entamoeba histolytica* parasite[§]

Juan David Ospina-Villa[1], Nancy Guillén[2], Cesar Lopez-Camarillo[3], Jacqueline Soto-Sanchez[1], Esther Ramirez-Moreno[1], Raul Garcia-Vazquez[1], Carlos A. Castañon-Sanchez[4], Abigail Betanzos[5], and Laurence A. Marchat[1*]

[1]*Instituto Politécnico Nacional – ENMH, Ciudad de México, Mexico*
[2]*Institut Pasteur, Unité d'Analyses d'Images Biologiques, Paris, France*
[3]*Universidad Autónoma de la Ciudad de México – Posgrado en Ciencias Genómicas, Ciudad de México, Mexico*
[4]*Hospital Regional de Alta Especialidad, Oaxaca, Mexico*
[5]*Cátedras, CONACYT, Departamento de Infectómica y Patogénesis Molecular, CINVESTAV-IPN, Ciudad de México, Mexico*

(Received Jun 27, 2017 / Revised Aug 16, 2017 / Accepted Aug 19, 2017)

The 25 kDa subunit of the Clevage Factor Im (CFIm25) is an essential factor for messenger RNA polyadenylation in human cells. Therefore, here we investigated whether the homologous protein of *Entamoeba histolytica*, the protozoan responsible for human amoebiasis, might be considered as a biochemical target for parasite control. Trophozoites were cultured with bacterial double-stranded RNA molecules targeting the *EhCFIm25* gene, and inhibition of mRNA and protein expression was confirmed by RT-PCR and Western blot assays, respectively. *EhCFIm25* silencing was associated with a significant acceleration of cell proliferation and cell death. Moreover, trophozoites appeared as larger and multinucleated cells. These morphological changes were accompanied by a reduced mobility, and erythrophagocytosis was significantly diminished. Lastly, the knockdown of *EhCFIm25* affected the poly(A) site selection in two reporter genes and revealed that *EhCFIm25* stimulates the utilization of downstream poly(A) sites in *E. histolytica* mRNA. Overall, our data confirm that targeting the polyadenylation process represents an interesting strategy for controlling parasites, including *E. histolytica*. To our best knowledge, the present study is the first to have revealed the relevance of the cleavage factor CFIm25 as a biochemical target in parasites.

Keywords: amoebiasis, gene knockdown, polyadenylation, protozoan parasite, virulence

*For correspondence. E-mail: lmarchat@gmail.com; lmarchat@ipn.mx; Tel.: +52-55 5729-6300 (ext. 55543)
[§]Supplemental material for this article may be found at http://www.springerlink.com/content/120956.

Introduction

The polyadenylation of pre-messenger mRNA (pre-mRNA) at the 3′-end is a fundamental process for gene expression regulation in eukaryotic cells; it establishes an important connection with transcription (Batt *et al*., 1994), confers stability to mRNA (Barnhart *et al*., 2013), plays a role in mRNA nuclear export, streamlines translation (Colgan and Manley 2016), and protects mRNA from degradation (Tourrière *et al*., 2002). Alterations in polyadenylation have been related with several human illnesses like α and β thalassemia, neonatal diabetes, Fabry disease, and cancer (Curinha *et al*., 2014), as well as with lethal defects in yeast (Wang *et al*., 2005), demonstrating that this event is essential for accurate cell survival. The poly(A) tail formation requires the participation of protein complexes known as CPSF (Cleavage and Polyadenylation Specific Factor), CstF (Cleavage Stimulating Factor), CFIm and CFIIm (Cleavage Factor Im and IIm), as well as PAP Poly(A) Polymerase and PABPII Poly(A) Binding Protein, that bind to specific motifs in 3′-UTR. In human cells, the CFIm complex is a heterotetrameric complex formed by a homodimer of 25 kDa subunits interacting with two larger subunits (72, 68, or 59 kDa). Each CFIm25 subunit (also known as CPSF5 or NUDT21) binds to the UGUA motif and affinity is increased by interaction with the RRM domain of larger subunits (Yang *et al.,* 2011). The knockdown of CFIm25 protein affects the poly(A) site selection (Kubo *et al.,* 2006), the recruitment of polyadenylation factors to pre-mRNA 3′-end, and the cleavage and polyadenylation reactions (Brown and Gilmartin, 2003), which highlights the relevance of this subunit in poly(A) tail synthesis. Our search in the Unified Human Interactome database at http://www.unihi.org/ (Kalathur *et al*., 2013) showed that CFIm25 interacts with splicing factors (U2AF1, SF3B1, SNRNP70, and others), and export (NXF1) and transcription factors (GTF2F1, HSF4, TCERG1). Some of these interactions have been previously reported (De Vries *et al*., 2000; Awasthi and Alwine, 2003; Ingham *et al*., 2005; Vinayagam *et al*., 2011), confirming that CFIm25 establishes a functional link between the different molecular events of mRNA synthesis and processing.

We previously reported the polyadenylation machinery of *Entamoeba histolytica,* the protozoan parasite responsible for the human amoebiasis that affects 50 million individuals per year (Ralston and Petri, 2011). By extensive analyses of parasite genome sequences, we described conserved motifs in pre-mRNA 3′-ends, namely the poly(A) signal A(U/A)UU, and the U-rich and A-rich elements (Zamorano *et al*., 2008). We also identified polyadenylation factors that contain the functional domains described in homologous proteins in

eukaryotic cells (López-Camarillo *et al.*, 2005), suggesting that the polyadenylation process is conserved through evolution. Importantly, *E. histolytica* only has the subunit of 25 kDa (EhCFIm25) of the CFIm complex. EhCFIm25 binds to mRNA 3′UTR and this interaction involves the participation of conserved Leu135 and Tyr236 residues (Ospina-Villa *et al.*, 2015). Moreover, EhCFIm25 interacts with other polyadenylation factors, such as the poly(A) polymerase EhPAP (Pezet-Valdez *et al.,* 2013) and the transcriptional coactivator EhPC4 (our unpublished data) that has been recently related to virulence, DNA replication and multinucleation in *E. histolytica* (Hernández de la Cruz *et al.,* 2014, 2016). Altogether these data suggest a relevant role for EhCFIm25 in mRNA polyadenylation and other processes related to gene expression. The objective of the present work was to evaluate how *EhCFIm25* gene silencing affects *E. histolytica* trophozoites in order to determine the potential of this polyadenylation factor as a biochemical target for parasite control.

Materials and Methods

Cell cultures

E. histolytica trophozoites (strain HMI:IMSS) were grown at 37°C in TYI-S-33 medium supplemented with 20% bovine serum, 100 U/ml penicillin and 100 μg/ml streptomycin (Diamond *et al.*, 1978), and parasites were harvested during exponential growth phase for all experiments. RNAseIII-deficient *Escherichia coli* strain HT115 (rnc14:DTn10) was grown at 37°C in LB broth for plasmid construction or 2YT broth for dsRNA expression, in the presence of ampicillin (100 mg/ml) and tetracycline (10 mg/ml) (Takiff *et al.*, 1989).

Double-stranded RNA (dsRNA)-based *EhCFIm25* gene silencing

Expression of bacterial dsRNA and parasite soaking experiments were performed as described (Solis *et al.*, 2009). Briefly, a 342-bp fragment of the *EhCFIm25* gene was PCR amplified from the pRSET-*EhCFIm25* vector (Pezet-Valdez *et al.*, 2013) using pL4440EhCFIm25-S (5′-CCCCCCGGGGGAGAAGATGATCCTGTTGAAGG-3′) and pL4440EhCFIm25-AS (5′-CCCCTCGAGTTAACCATAAATCATAAGATACCTTG-3′) primers and cloned into *Sma*I and *Xho*I restriction sites of the pL4440 vector (Fig. 1A). PCR, restriction analysis and DNA sequencing were performed to verify the resulting pL4440-*EhCFIm25* plasmid. Then, competent *E. coli* HT115 cells were transformed with the pL4440-*EhCFIm25* plasmid and the expression of *EhCFIm25*-dsRNA was induced with 2 mM isopropyl β-D-1-thiogalactopyranoside (IPTG) for 4 h at 37°C. Then, bacterial pellet was mixed with 1 M ammonium acetate and 10 mM EDTA, incubated with phenol : chloroform : isoamyl alcohol (25 : 24 : 1) and centrifuged. The supernatant was mixed with isopropanol, cen-

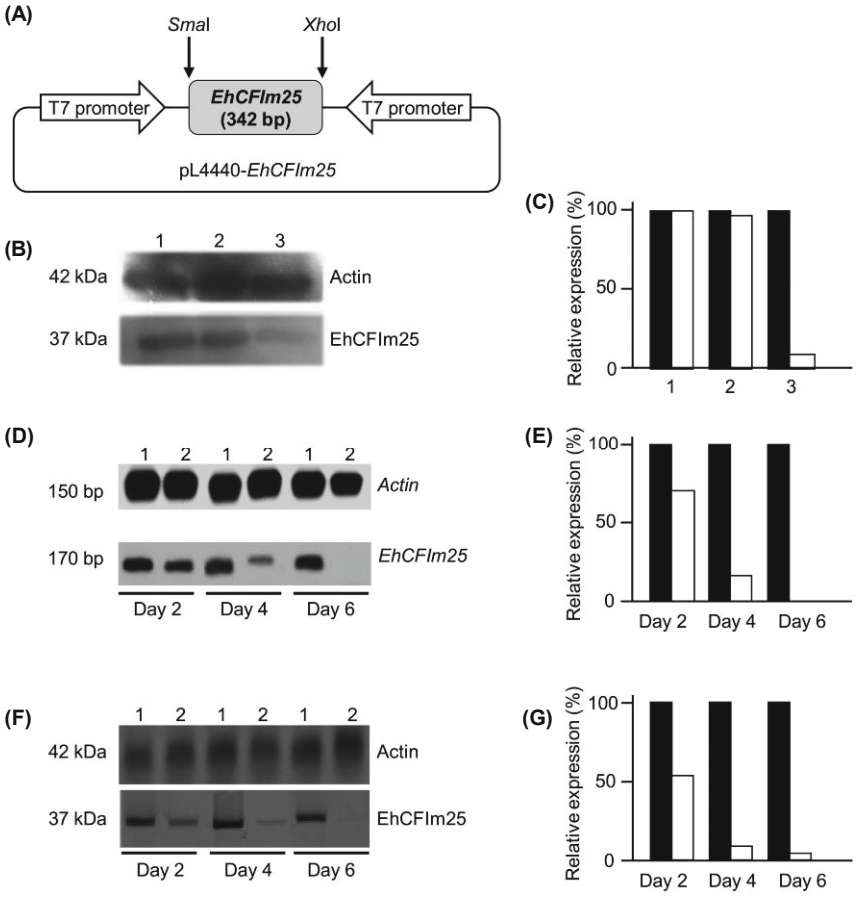

Fig. 1. Silencing of *EhCFIm25* gene expression in *E. histolytica* trophozoites exposed to *EhCFIm25*-dsRNA. (A) pL4440-*EhCFIm25* plasmid construct. (B) Immunodetection of EhCFIm25 protein expression by Western blot assay after seven days of the soaking experiment. Lanes: 1, trophozoites in standard conditions (control); 2, trophozoites exposed to *gfp*-dsRNA; 3, trophozoites exposed to *EhCFIm25*-dsRNA. (C) Densitometry analysis of bands in (B). Data corresponding to actin amount (black bar) were taken as 100% and used to determine the relative expression of EhCFIm25 (white bar) in the three experimental conditions. (D) *EhCFIm25* mRNA expression by RT-PCR assay on day 2, 4, and 6 of soaking experiment. Lanes: 1, control trophozoites; 2, trophozoites exposed to *EhCFIm25*-dsRNA). (E) Densitometry analysis of bands in (B). Data corresponding to *EhCFIm25* mRNA amount (black bar) in control trophozoites were taken as 100% to obtain the relative mRNA expression in cells treated with *EhCFIm25*-dsRNA (white bar). (F) Immunodetection of EhCFIm25 protein expression by Western blot assay on day 2, 4, and 6 of soaking experiment. Lanes: 1, control trophozoites; 2, trophozoites exposed to *EhCFIm25*-dsRNA. (G) Densitometry analysis of bands in (F). Data corresponding to EhCFIm25 amount in control cells were taken as 100% and used to determine the relative expression of EhCFIm25 in cells grown with *EhCFIm25*-dsRNA. Actin was used as loading control.

trifuged, and the nucleic acid pellet was washed with 70% ethanol. DNase I (Invitrogen) and RNase A (Ambion) were added to eliminate ssRNA and dsDNA molecules, *EhCFIm25*-dsRNA was washed again with isopropanol and ethanol, analyzed by agarose gel electrophoresis and quantified by spectrophotometry. Lastly, purified *EhCFIm25*-dsRNA molecules were added to trophozoites (5.0×10^4) in TYI-S-33 complete medium to a final concentration of 100 µg/ml and cultures were incubated at 37°C for seven days. Cells growing in standard conditions (without dsRNA) and exposed to *gfp*-dsRNA obtained from the pL4440-*gfp* (green-fluorescent protein gene) construct (Solis *et al.*, 2009) were used as controls.

RT-PCR amplification

Total RNA of *E. histolytica* trophozoites was purified by the Trizol reagent (Invitrogen). cDNA was obtained from 1 µg of RNA using 200 ng of oligo (dT) primer (Bio Synthesis Inc.) and 200 U of M-MLV Reverse Transcriptase (Invitrogen) for 50 min at 37°C. RNA was eliminated by adding *E. coli* Ribonuclease H (2 U; ThermoFisher Scientific) for 20 min at 37°C.The volume corresponding to 100 ng of cDNA was mixed with *EhCFIm25* sense (5′-TGGAGAAGATGA TCCTGTTGAAG-3′) and antisense (5′-TCTTTGACTTG ACTTACATGAACTG-3′) primers (10 µM each) and PCR was performed using TaqDNA polymerase (ThermoFisher Scientific) in a C1000^{TM} Thermal Cycler (Applied Biosystem). The *actin* gene was used as control. Amplified products were separated through 12% polyacrylamide-TBE gel electrophoresis, stained with GelRed (Biotium), observed in a Gel-Doc apparatus (Bio-Rad) and quantified using the ImageJ processing program (Schneider *et al.*, 2012). Data corresponding to *EhCFIm25* gene expression in control trophozoites were taken as 100% to obtain the relative mRNA expression in cells exposed to *EhCFIm25*-dsRNA.

Western blot analysis

Total proteins (60 µg) of *E. histolytica* trophozoites were separated by 10% SDS-PAGE and electrotransferred to a nitrocellulose membrane following standard protocols. After staining with Ponceau, the endogenous EhCFIm25 protein was detected by incubation with anti-EhCFIm25 antibodies (1:500) for 2 h at room temperature (RT) (Pezet-Valdez *et al.*, 2013). Blots were washed five times with PBS 1 X pH 7.4 and incubated with anti-rabbit IgG conjugated to horseradish peroxidase (1:2000;ThermoFisher Scientific) for 2 h at room temperature (RT). Actin was used as control. Bands were developed using the ECL Plus Western blotting detection system (Amersham) and quantified using the ImageJ processing program (Schneider *et al.*, 2012). In some experiments, data corresponding to actin expression were taken as 100% and used to determine the relative expression of EhCFIm25 in control trophozoites (without dsRNA or with *gfp*-dsRNA) and cells exposed to *EhCFIm25*-dsRNA. In others, data corresponding to EhCFIm25 expression in control cells without dsRNA were taken as 100% and used to determine the relative expression of EhCFIm25 in cells exposed to *EhCFIm25*-dsRNA.

Cell proliferation and viability assays

A 10 µl aliquot of *E. histolytica* cultures was taken each day and cells were counted in a Neubauer chamber for seven days during the soaking experiments. Simultaneously, living cells were identified in a Trypan blue test. Experiments were performed twice in triplicate. Results were expressed as mean ± standard deviation (SD).

Morphology, area and velocity of trophozoites

E. histolytica trophozoites were observed on an Eclipse 80i microscope (Nikon), pictures and videos were obtained and analyzed by the Icy software that provides the resources to visualize, annotate and quantify bioimaging data (De Chaumont *et al.*, 2012). Trophozoites (approximately 400 cells) were examined through the active contours tool to determine the cellular area (μm^2), and data were expressed as mean ± SD. On the other hand, 60 videos of 2 min were analyzed with the Track Manager Plugin tool and speed was expressed as pixels *per* frame of 2 sec.

Immunofluorescence assays

Trophozoites were grown on coverslips, washed five times with PBS pH 6.8, fixed with 4% paraformaldehyde for 1 h at 37°C and permeabilized with 0.2% Triton X-100 for 10 min at RT. After blocking with 10% fetal bovine serum (FBS) for 1 h at RT, trophozoites were stained for 5 min with 2.5 µg/ml DAPI (4′,6-diamidino-2-phenylindole) (Zymed). Cells were mounted using Vectashield (Vector laboratories) and analyzed in a confocal microscope (Leica TCS_SP5_MO) through *Z*-stack sections of 0.5 mm in *xy*-planes. In all cases, 80 cells were examined per condition.

Cell migration assays

E. histolytica trophozoites (10^4) were placed in 100 µl of serum-free TYI-S-33 medium in the upper compartment of the Transwell chamber (Corning) with 6.5 mm diameter and 8 µm pore size polycarbonate membrane; the lower chamber was loaded with 650 µl of complete TYI-S-33 medium. After 3 h at 37°C, the number of trophozoites that have migrated into the lower chamber was counted in a Neubauer chamber. Experiments were performed twice in triplicate and results were reported as mean ± SD.

Erythrophagocytosis assays

Human whole blood diluted in Hayem reagent (1:200) was kept in gentle shake for 5 min. After leukocytes lysis, intact erythrocytes were counted in a Neubauer chamber and mixed with *E. histolytica* trophozoites (100:1) for 5, 10, and 15 min at 37°C. The erythrophagocytosis process was stopped by addition of distilled cold water (1 ml). Cells were centrifuged at 1,500 rpm for 5 min, the pellet was mixed with 2 ml of 3,3-diaminobenzidine (2 mg/ml) and 0.2% H_2O_2 for 30 min at 37°C. After centrifugation, cells were observed on an Eclipse TS100 microscope (Nikon). The number of erythrocytes per amoeba was determined in 100 randomly selected trophozoites. Experiments were performed twice in triplicate and results were expressed as mean ± SD.

Polyadenylation site selection assay

The thiorredoxin (EHI_021560) and *60S ribosomal protein L7* (EHI_025830) genes were selected since RNA-Seq experiments showed that they contain two alternative poly(A) sites (Hon *et al.*, 2013; Guillen, pers. commun.). Total RNA of *E. histolytica* trophozoites was reverse transcribed with oligo(dT) primer as described above. Then, the 3′ end of each gene was PCR amplified using two pairs of primers that target the proximal or distal poly(A) sites. For the thiorredoxin gene, we designed the EHI_021560 sense (5′-TTCCCATCC TTTTTAACTTT-3′) and antisense 1 (5′-TGAAAAAGTTA TTATTTAAAGTT-3′) primers that produce a 72 bp fragment, while the EHI_021560 sense and antisense 2 (5′-AA TAAAATAAATTTGTTATTAATTT-3′) oligonucleotides produce a 102 bp fragment. The EHI_025830 sense (5′-AT TTTAACGACTTTTCTTATT-3′) and antisense 1 (5′-TCC AACAACCATTTCAATT-3′) primers produce a 78 bp fragment of the *60S ribosomal protein L7* mRNA 3′ end, while the EHI_025830 sense and antisense 2 (5′-GATAATAATA AATTACTAGTAA-3′) primers produce a 127 bp fragment (Fig. 4A and B). The *actin* gene was used as loading control. PCR was performed as described above using 100 ng of cDNA. Amplified products were separated through 2% polyacrylamide-TBE gel electrophoresis, stained with GelRed (Biotium), observed in a Gel-Doc apparatus (Bio-Rad) and quantified using the ImageJ processing program (Schneider *et al.*, 2012). For each band, pixels corresponding to cells growing in standard conditions were taken as 100% and used to normalize data obtained from EhCFIm25-silenced trophozoites.

Results

Silencing of *EhCFIm25* affects proliferation, viability and morphology of trophozoites

To evaluate the functional relevance of EhCFIm25 in *E. histolytica*, we silenced the *EhCFIm25* gene expression using

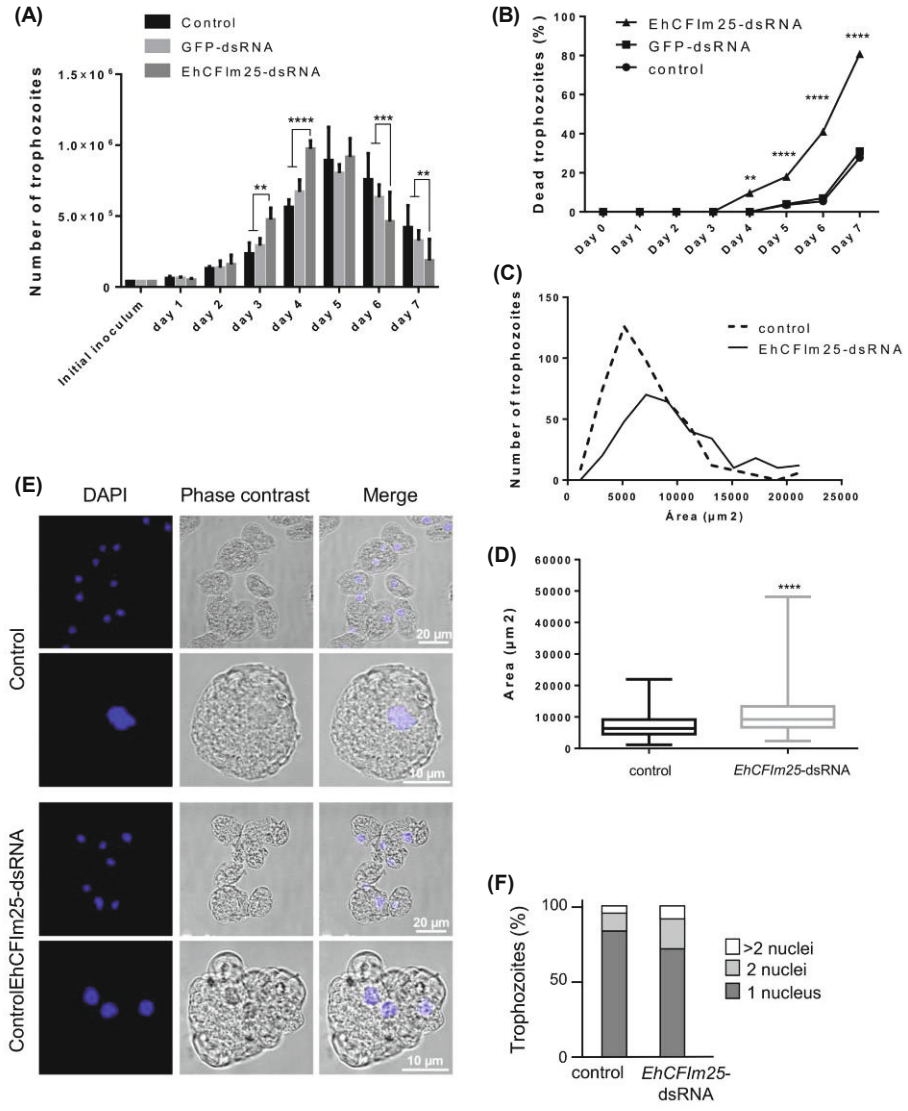

Fig. 2. Effect of *EhCFIm25* silencing on cell proliferation, viability, and morphology of *E. histolytica* trophozoites. (A) and (B) Trophozoites were exposed to *EhCFIm25*-dsRNA (100 µl/ml) for seven days at 37°C. Each day, cell number was determined (A) and viability was assessed in a Trypan blue assay (B). Data were compared to those obtained from trophozoites growing in standard conditions (control) and exposed to *gfp*-dsRNA using the two-way ANOVA test. (C) and (D) Cellular area was determined using the active contour tool of the Icy software. Data in (D) were analyzed using the *t*-test. (E) Fluorescence and confocal microscopy assays showing nuclei in trophozoites stained with DAPI. (F) Number of nuclei per trophozoites. $^{**}P < 0.01$; $^{***}P < 0.001$ and $^{****}P < 0.0001$.

EhCFIm25-dsRNA. For this purpose, we PCR-amplified a 342 bp fragment of the *EhCFIm25* gene and cloned it into the pL4440 plasmid (Fig. 1A). Sequencing of the resulting pL4440-*EhCFIm25* plasmid confirmed the identity of the cloned fragment (data not shown). Then, *EhCFIm25*-dsRNA was expressed in bacteria, purified, and added to parasite cultures at the final concentration of 100 µg/ml. Western blot assays evidenced the efficient silencing (~90%) of *EhCFIm25* gene expression on day 7, relative to cells growing without dsRNA. Similarly, ingestion of unrelated dsRNA, i. e. *gfp*-dsRNA that does not have a natural target in parasite genome, had no effect on EhCFIm25 expression. Actin amount remained unchanged in the three experimental conditions, indicating that *EhCFIm25*-dsRNA specifically targeted the *EhCFIm25* gene expression (Fig. 1B and C). Then, we evaluated *EhCFIm25* gene expression throughout a 6 day-period. Results showed that *EhCFIm25* gene transcription was reduced by ~30%, ~80%, and ~100% on days 2, 4, and 6, respectively, relative to cells without treatment, whereas actin expression was not significantly affected throughout the experiment (Fig. 1D and E). Accordingly, the amount of EhCFIm25 was also reduced by ~50%, ~90%, and ~95% on day 2, 4, and 6, respectively, while actin amount remained almost constant (Fig. 1F and G).

To elucidate the impact of *EhCFIm25* gene silencing on trophozoites, we first evaluated cell proliferation and death throughout a week. Growth kinetic curves showed that both control groups have a similar behavior, confirming that unrelated dsRNA that do not target parasite genes, do not have any effect on trophozoites. Interestingly, cultures exposed to *EhCFIm25*-dsRNA exhibited an accelerated proliferation on days 3 and 4, when compared with both control groups; then, proliferation slowed down on day 5, before being drastically reduced on days 6 and 7 (Fig. 2A). Accordingly, these cultures presented a significantly higher proportion of dead parasites from day 4 (~10% dead cells *versus* none in both control groups, $P \leq 0.0001$). On day 7, dead cells represented about 80% of the population, while we found only ~30% dead cells in both control groups ($P \leq 0.0001$) (Fig. 2B). Statistical analyses did not evidence significant differences between both control groups described above; hence, we considered trophozoites growing in standard conditions (without dsRNA) as control for the rest of the experiments.

We noticed morphological changes in EhCFIm25-silenced trophozoites throughout the experiment; therefore, we decided to quantify cellular size at 96 h, when most cells were still alive although the EhCFIm25 amount was significantly reduced, using the active contours tool of the Icy software. As shown in Fig. 2C, cellular area showed a Gaussian distribution in both conditions. However, the curve corresponding to cells exposed to *EhCFIm25*-dsRNA was shifted to the right. Particularly, the mean cellular area significantly increased from 7,044 ± 165.9 µm^2 (n = 444) in control cells up to 11,402 ± 390.6 µm^2 (n = 354) in trophozoites exposed to *EhCFIm25*-dsRNA ($P \leq 0.0001$) (Fig. 2D). In addition, confocal microscopy experiments evidenced that these larger trophozoites contain a higher amount of nuclei than control cells; notably, the number of cells with two or more nuclei significantly increased from 18.6% in control cells up to 27.6% in EhCFIm25-silenced trophozoites (Fig. 2E and F).

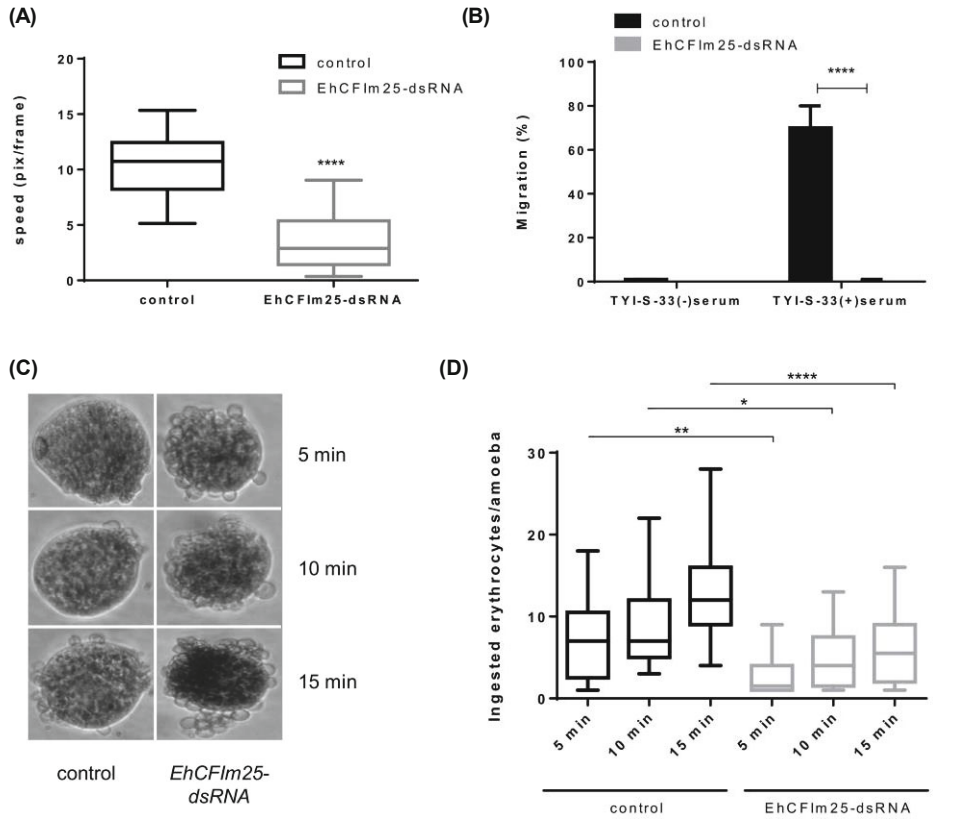

Fig. 3. Effect of *EhCFIm25* silencing on speed, migration and erythrophagocytosis in *E. histolytica* trophozoites. (A) Speed. Trophozoites were observed through an Eclipse 80i microscope and videos were processed using the track manager plugin tool of the Icy software. Data were analyzed using the *t*-test. (B) Migration assay using the transwell chamber (Corning). Data were analyzed using the two-way ANOVA test. (C) and (D) Erythrophagocytosis assay. (C) Representative photographs showing erythrocytes engulfed by trophozoites at 5, 10, and 15 min of interaction. (D) Number of engulfed erythrocytes per trophozoites. Data were analyzed using the one-way ANOVA test. *$P < 0.05$; **$P < 0.01$; and ****$P < 0.0001$.

The hypothesis that these observations could result from silencing of other amoeba proteins was rejected since BLAST sequence analyses showed that neither the sense strand nor the complementary strand of *EhCFIm25*-dsRNA display homology with parasite genes.

Silencing of *EhCFIm25* affects mobility and phagocytic capacity of trophozoites

We observed that EhCFIm25-silenced trophozoites seem to move slower. A more detailed examination of living cells revealed that parasites grown in standard conditions make the classic amoeboid movements to move on the microscopic slide (Supplementary data Video S1 and S3). In contrast, most trophozoites exposed to *EhCFIm25*-dsRNA (~80%) undergo uncontrolled movements, turning on themselves, without being able to successfully move on the slide (Supplementary data Video S3 and S4). To quantify these observations, we analyzed the speed of trophozoites at 48 h by using the track manager tool of the Icy software. Results showed that velocity was significantly reduced from 10.52 ± 0.3542 pixels/frame in control cells to 3.500 ± 0.3160 pixels/frame in EhCFIm25-silenced cells ($P \leq 0.0001$) (Fig. 3A). We also used the transwell chamber system to evaluate the migration of trophozoites. As shown in Fig. 3B, 70 ± 10 control cells were able to migrate to the lower compartment, whereas only 0.33 ± 0.577 migratory cells were found in cultures treated with *EhCFIm25*-dsRNA.

Besides mobility and migration, phagocytosis is another hallmark of parasite virulence. Therefore, we evaluated the erythrophagocytosis capacity of EhCFIm25-silenced trophozoites at 48 h. Microscopic evaluation showed that EhCFIm25 knockdown induced a significant reduction in the number of ingested red blood cells, from 7.414 ± 5.082, 8.621 ± 4.953, and 13.08 ± 5.607 in control cells, to 2.967 ± 2.834, 4.862 ± 3.672, and 6.156 ± 4.341 in parasites exposed to *EhCFIm25*-dsRNA, after 5, 10, and 15 min of interaction (Fig. 3C and D).

Silencing of *EhCFIm25* affects the poly(A) site selection

We previously reported that EhCFIm25 is an RNA binding protein that interacts with other polyadenylation factors (Pezet-Valdez *et al.,* 2013; Ospina-Villa *et al.,* 2015). To gain insights into its function in the polyadenylation process, here we evaluated its relevance for the poly(A) site selection. For this purpose, we selected two genes with multiple poly(A) sites from RNA-Seq data (Hon *et al.,* 2013; Guillen, pers. commun.) and designed primer pairs that allowed the specific amplification of fragments with different sizes according to the poly(A) site present in mRNA corresponding to each gene (Fig. 4A and B).In control trophozoites, the presence of the 72 and 102 bp bands confirmed that both proximal and distal poly(A) sites of the *thioredoxin* gene were selected. However, the amount of the smaller band was about 2.5-fold augmented in trophozoites exposed to *EhCFIm25*-dsRNA, whereas the amount of the larger band was almost the same, suggesting that the utilization of the proximal poly(A) site was increased in EhCFIm25-silenced cells. The functionality of both polyadenylation sites in the *60S ribosomal protein L7* gene was also confirmed by the amplification of the 78 and 118 bp bands. Similarly, we observed a 2-fold increase in the amount of the smaller band in the absence of EhCFIm25, indicating that the selection of proximal poly(A) site was favored (Fig. 4C and D). In control experiments, actin expression was constant in both control and silenced trophozoites, confirming that differences described above were significant (Fig. 4E).

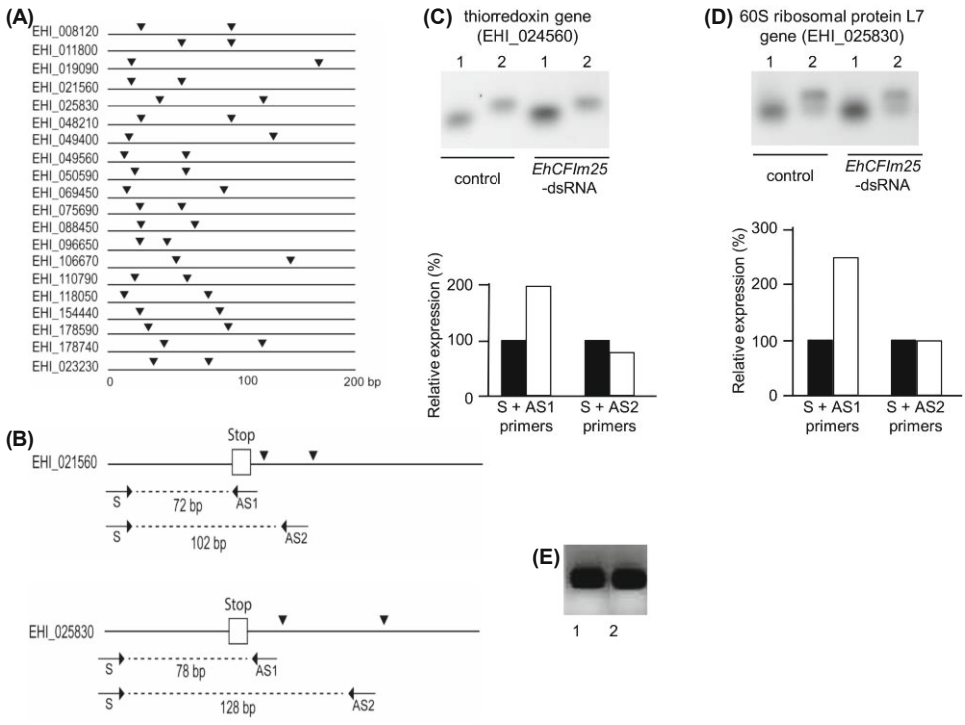

Fig. 4. Effect of *EhCFIm25* silencing on poly(A) site selection in *E. histolytica* trophozoites. (A) Schematic representation of 3′UTR of 20 genes with two experimentally determined poly(A) sites (Hon *et al.,* 2013; Guillen, pers. commun.). Arrowhead, poly(A) site. (B) Design of primers for the amplification of 3′UTR of *thioredoxin* and *60S ribosomal protein L7* genes according to the poly(A) site selected. S, sense primer; AS, antisense primer; box, stop codon; arrowhead, poly(A) site. (C) and (D) Upper panel, RT-PCR amplification of mRNA 3′end of the *thioredoxin* (C) and *60S ribosomal protein L7* (D) genes using S and AS1 primers to target the proximal poly(A) sites (lane 1), and S and AS2 primers for the distal poly(A) sites (lane 2), in control and EhCFIm25-silenced trophozoites. Lower panel, densitometry analysis of bands in upper panels. For each band, pixels corresponding to control cells were taken as 100% and used to normalize data obtained from EhCFIm25-silenced trophozoites. (E) RT-PCR amplification of actin used as control. Lanes: 1, control cells; 2, EhCFIm25-silenced trophozoites.

Discussion

We describe here for the first time that the polyadenylation factor EhCFIm25 represents a potential biochemical target for *E. histolytica* trophozoites control since knockdown of the *EhCFIm25* gene affected cell proliferation, mobility, and erythrophagocytosis, probably as a result of alterations in mRNA polyadenylation.

The dsRNA soaking method described by Solis *et al.* (2009) is a specific, reproducible, fast, and easy to perform protocol for silencing gene expression in *E. histolytica*. Consistently, a significant down regulation of EhCFIm25 transcript and protein amount was observed from day 2 in trophozoites exposed to *EhCFIm25*-dsRNA expressed in bacteria. The inhibition of gene expression was maintained throughout seven days, reaching up to ~90%, indicating that the silencing effect of a single inoculation of *EhCFIm25*-dsRNA was persistent and irreversible in our experimental conditions. In contrast, siRNA only produced a 50% inhibition of CFIm25 expression at 60 h in human cells and expression were almost totally recovered after 156 h (Kubo *et al.,* 2006).

EhCFIm25 inhibition produced alterations in cell growth, namely an accelerated cell proliferation associated with an increased cell death, suggesting that *E. histolytica* trophozoites were not able to fully overcome critical defects resulting from *EhCFIm25* silencing. These data also revealed that EhCFIm25 is essential for accurate parasite survival. In contrast, CFIm25 knockdown had no effect on morphology, cell viability, and proliferation in rat pheochromocytoma PC12 (Fukumitsu *et al*., 2012) and HeLa cells (Kubo *et al*., 2006). We hypothesize that these contradicting observations might be related to the fact that the 25 kDa polypeptide is the only CFIm subunit in *E. histolytica.* It is possible that the larger subunits of the heterotetrameric CFIm complex rescue the functions of the 25 kDa subunit in polyadenylation and other molecular events in higher eukaryotes. Indeed, the independent knockdown of each subunits, significantly altered the formation of the poly(A) tail in HeLa cells, demonstrating that both small and large subunits are essential components of CFIm (Kim *et al*., 2010).

Interestingly, EhCFIm25 knockdown was associated with an increase in size and nuclei number, and a reduction in virulence properties (cell mobility and erythrophagocytosis). An increase in cell proliferation and the formation of giant multinucleated cells has also been observed in trophozoites overexpressing EhPC4 (Hernández de la Cruz *et al*., 2016), a multifunctional factor that modulates transcription initiation and termination, as well as 3′ end processing, through its interaction with distinct proteins in higher eukaryotic cells (Sikorski *et al*., 2011). In *E. histolytica*, the upregulation of EhPC4 induced migration of trophozoites and destruction of intestinal host cells, through the induction of the 16-kDa actin-binding protein EhABP16 (Hernández de la Cruz *et al*., 2014). Altogether, these studies suggest that polyadenylation factors regulate *E. histolytica* virulence properties by modulating, directly or indirectly, the expression of genes involved in cell mobility, erythrophagocytosis and destruction of host intestinal cells. In the pathogenic process of *Cryptococcus neoformans*, the formation of giant and polynucleated cells allows it to avoid phagocytosis by host mononuclear cells, and resist to oxidative and nitrosative stress (Okagaki *et al*., 2010). However, the molecular mechanisms linking these morphological changes with virulence still need to be determined in *E. histolytica*. Nevertheless, with a view to the future clinical applications for EhCFIm25 silencing, it is important to keep in mind that *EhCFIm25*-dsRNA strands do not display homology with any human genes, which suggests that EhCFIm25 silencing could represent a mean of

Table 1. Cellular processes corresponding to *E. histolytica* genes with two poly(A) sites

mRNA ID*	Description	Cellular process
EHI_008120	Uncharacterized protein	ND
EHI_011800	Uncharacterized protein	ND
EHI_019090	Uncharacterized protein	ND
EHI_021560	Thioredoxin putative	Oxidation/reduction
EHI_025830	*60S ribosomal protein L7* putative	Translation
EHI_048210	splicing factor arginine serine-rich putative	Splicing
EHI_049400	chaperone proteinDNAJ putative	Protein folding
EHI_049560	Uncharacterized protein	ND
EHI_050590	Uncharacterized protein	ND
EHI_069450	Uncharacterized protein	ND
EHI_075690	Uncharacterized protein	ND
EHI_088450	Inositol polyphosphate 5-phosphatase putative	Signaling pathways
EHI_096650	Histone H3 putative	DNA compaction
EHI_106670	Calcineurin B subunit putative	Calcium ion binding
EHI_110790	Zinc finger domain containing protein	Cell cycle
EHI_118050	Coatomer alpha subunit putative	Intracellular transport
EHI_154440	Uncharacterized protein	ND
EHI_178590	Histone RNA hairpin-binding protein putative	mRNA binding
EHI_178740	Clathrin adaptor complex small chain putative	Protein transport
EHI_023230	Histone H4	DNA binding

*http://amoebadb.org/amoeba/; ND, not determined.

controlling *E. histolytica* survival without affecting the polyadenylation process in host cells.

We have previously reported that EhCFIm25 is an RNA binding protein that interacts with other polyadenylation and transcription factors (Pezet-Valdez *et al.*, 2013; our unpublished data). Here, we showed that EhCFIm25 controls the efficient selection of distal (or downstream) poly(A) sites in *E. histolytica* transcripts. In human cells, alternative polyadenylation is emerging as a common mechanism to control gene expression and CFIm25 has a key role in this event (Kubo *et al.*, 2006; Kim *et al.*, 2010). The mean length of mRNA 3′UTRs is ~700 nt and ~69.1% of genes have multiple polyadenylation sites (Derti *et al.*, 2012). The selection of proximal poly(A) sites results in the elimination of RNA motifs that are important for coding capacity, localization, translation efficiency and stability of transcripts (Gilmartin, 2005). In higher eukaryotic cells, mRNA turnover depends on AU-rich elements (AURE) (Caput *et al.*, 1986), RNA binding proteins mainly represented by Hu (Fan and Steitz, 1998) and AUF1 (Zhang *et al.*, 1993), and structure constraints such as stem-loop motifs (Klaff *et al.*, 1996). Moreover, 3′UTR contain complementary sequences for miRNAs (Vasudevan *et al.,* 2007). In *E. histolytica*, 3′UTR are short (~21 nt); only a small proportion of genes (1.9 to 2.4%) have long-range heterogeneity of poly(A) site, suggesting a limited impact of alternative polyadenylation on gene expression regulation. A stringent bioinformatic analysis of transcriptome data obtained from RNA-Seq led to the identification of 20 genes with two polyadenylation sites (Hon *et al.*, 2013). Any changes in polyadenylation factors would likely alter the processing of transcript 3′-end and therefore gene expression. Then, the use of proximal poly(A) sites in EhCFIm25-silenced trophozoites may result in the loss of RNA sequences that are important for mRNA stability and translation.

Although 3′UTR have not been extensively studied in *E. histolytica*, some reports indicate their relevance for gene expression regulation (De *et al.*, 2006; Lopez-Camarillo *et al.*, 2003; Hon *et al.*, 2013). Interestingly, genes with alternative polyadenylation sites have a huge impact on global gene expression in *E. histolytica* since most of them participate in DNA condensation, DNA binding, translation, splicing, mRNA binding, protein folding and protein transport. Other genes are related with signaling, oxidation/reduction, calcium ion binding, cell cycle and intracellular transport (Table 1). We hypothesize that the upstream shift in poly(A) site selection of the corresponding transcripts may contribute to the phenotype of EhCFIm25-silenced trophozoites. Future experiments will be performed to describe the transcriptome in EhCFIm25-depleted cells and measure the impact of EhCFIm25 silencing on gene expression in *E. histolytica*. Moreover, it would be worth performing RNA-Seq experiments to identify genes whose 3′-end formation relies on EhCFIm25 and confirm the relevance of alternative polyadenylation in this human pathogen.

In conclusion, our data confirm that targeting the polyadenylation process represents an interesting strategy for controlling parasites, including *E. histolytica*. They also showed that the polyadenylation factor EhCFIm25 is associated with events related to parasite proliferation, survival, and virulence, through its participation in the poly(A) site selection. These data prompt us to propose that EhCFIm25 may represent an interesting biochemical target in this human pathogen.

Acknowledgements

This work was supported by Mexico-France grants (SEP-CONACYT-ANUIES [249554] and ECOS NORD [M14S02]), and Mexican grants from CONACyT (178550) and SIP-IPN (SIP20170969). ERM and LAM were supported by COFAA-IPN. JDOV and RGV were scholarship recipients from Mexican BEIFI-IPN and CONACyT programs.

References

Awasthi, S. and Alwine, J.C. 2003. Association of polyadenylation cleavage factor I with U1 snRNP. *RNA*. **9**, 1400–1409.

Barnhart, M.D., Moon, S.L., Emch, A.W., Wilusz, C.J., and Wilusz, J. 2013. Changes in cellular mRNA stability, splicing and polyadenylation through HuR protein sequestration by a cytoplasmic RNA virus. *Cell Rep.* **5**, 909–917.

Batt, D.B., Luo, Y., and Carmichael, G.G. 1994. Polyadenylation and transcription termination in gene constructs containing multiple tandem polyadenylation signals. *Nucleic Acids Res.* **22**, 2811–2816.

Brown, K.M. and Gilmartin, G.M. 2003. A mechanism for the regulation of pre-mRNA 3′ processing by human cleavage factor I_m. *Mol. Cell* **12**, 1467–1476.

Caput, D., Beutler, B., Hartog, K., Thayer, R., Brown-Shimer, S., and Cerami, A. 1986. Identification of a common nucleotide sequence in the 3′-untranslated region of mRNA molecules specifying inflammatory mediators. *Proc. Natl. Acad. Sci. USA* **83**, 1670–1674.

Colgan, D.F. and Manley, J.L. 2016. Mechanism and regulation of mRNA polyadenylation. *Genes Dev.* **11**, 2755–2766.

Curinha, A., Braz, S.O., Pereira-Castro, I., Cruz, A., and Moreira, A. 2014. Implications of polyadenylation in health and disease. *Nucleus* **5**, 508–519.

De, S., Pal, D., and Ghosh, S.K. 2006. *Entamoeba histolytica*: computational identification of putative microRNA candidates. *Exp. Parasitol.* **113**, 239–243.

De Chaumont, F., Dallongeville, S., Chenouard, N., Hervé, N., Pop, S., Provoost, T., Meas-Yedid, V., Pankajakshan, P., Lecomte, T., Le Montagner, Y., *et al.* 2012. Icy: an open bioimage informatics platform for extended reproducible research. *Nat. Methods* **9**, 690–696.

De Vries, H., Rüegsegger, U., Hübner, W., Friedlein, A., Langen, H., and Keller, W. 2000. Human pre-mRNA cleavage factor II_m contains homologs of yeast proteins and bridges two other cleavage factors. *EMBO J.* **19**, 5895–5904.

Derti, A., Garrett-Engele, P., Macisaac, K.D., Stevens, R.C., Sriram, S., Chen, R., Rohl, C.A., Johnson, J.M., and Babak, T. 2012. A quantitative atlas of polyadenylation in five mammals. *Genome Res.* **22**, 1173–1183.

Diamond, L.S., Harlow, D.R., and Cunnick, C.C. 1978. A new medium for the axenic cultivation of *Entamoeba histolytica* and other *Entamoeba*. *Trans. R. Soc. Trop. Med. Hyg.* **72**, 431–432.

Fan, X.C. and Steitz, J.A. 1998. Overexpression of HuR, a nuclear-cytoplasmic shuttling protein, increases the *in vivo* stability of ARE-containing mRNAs. *EMBO J.* **17**, 3448–3460.

Fukumitsu, H., Soumiya, H., and Furukawa, S. 2012. Knockdown of pre-mRNA cleavage factor I_m 25 kDa promotes neurite outgrowth. *Biochem. Bioph. Res. Co.* **425**, 848–853.

Gilmartin, G.M. 2005. Eukaryotic mRNA 3′ processing: a common means to different ends. *Genes Dev.* **19**, 2517–2521.

Hernández de la Cruz, O., Marchat, L.A, Guillén, N., Weber, C., López-Rosas, I., Díaz-Chávez, J. Herrera, L., Rojo-Domínguez, A., Orozco, E., and López-Camarillo, C. 2016. Multinucleation and polykaryon formation is promoted by the EhPC4 transcription factor in *Entamoeba histolytica*. *Sci. Rep.* **6**, 19611.

Hernández de la Cruz, O., Muñiz-Lino, M., Guillén, N., Weber, C., Marchat, L.A, López-Rosas, I. Ruíz-García, E., Astudillo-de la Vega, H., Fuentes-Mera, L., Álvarez-Sánchez, E., *et al.* 2014. Proteomic profiling reveals that EhPC4 transcription factor induces cell migration through up-regulation of the 16-kDa actin-binding protein EhABP16 in *Entamoeba histolytica*. *J. Proteomics* **111**, 46–58.

Hon, C.C., Weber, C., Sismeiro, O., Proux, C., Koutero, M., Deloger, M., Das, S., Agrahari, M., Dillies, M.A., Jagla, B., *et al.* 2013. Quantification of stochastic noise of splicing and polyadenylation in *Entamoeba histolytica*. *Nucleic Acids Res.* **41**, 1936–1952.

Ingham, R.J., Colwill, K., Howard, C., Dettwiler, S., Lim, C.S.H., and Yu, J. 2005. WW domains provide a platform for the assembly of multiprotein networks. *Mol. Cell. Biol.* **25**, 7092–7106.

Kalathur, R.K.R., Pinto, J.P., Hernández-Prieto, M.A., Machado, R.S.R., Almeida, D., Chaurasia, G., and Futschik, M.E. 2013. UniHI 7: an enhanced database for retrieval and interactive analysis of human molecular interaction networks. *Nucleic Acids Res.* **42**, D408–D414.

Kim, S., Yamamoto, J., Chen, Y., Aida, M., Wada, T., Handa, H., and Yamaguchi, Y. 2010. Evidence that cleavage factor I_m is a heterotetrameric protein complex controlling alternative polyadenylation. *Genes Cells* **15**, 1003–1013.

Klaff, P., Riesner, D., and Steger, G. 1996. RNA structure and the regulation of gene expression. *Plant Mol. Biol.* **32**, 89–106.

Kubo, T., Wada, T., Yamaguchi, Y., Shimizu, A., and Handa, H. 2006. Knock-down of 25 kDa subunit of cleavage factor I_m in Hela cells alters alternative polyadenylation within 30-UTRs. *Nucleic Acids Res.* **34**, 6264–6271.

López-Camarillo, C., Luna-Arias, J.P., Marchat, L.A., and Orozco, E. 2003. EhPgp5 mRNA stability is a regulatory event in the *Entamoeba histolytica* multidrug resistance phenotype. *J. Biol. Chem.* **278**, 11273–11280.

López-Camarillo, C., Orozco, E., and Marchat, L.A. 2005. *Entamoeba histolytica*: Comparative genomics of the pre-mRNA 3′ end processing machinery. *Exp. Parasitol.* **110**, 184–190.

Okagaki, L.H., Strain, A.K., Nielsen, J.N., Charlier, C., Baltes, N.J., Chrétien, F., Heitman, F., Dromer, F., and Nielsen, K. 2010. Cryptococcal cell morphology affects host cell interactions and pathogenicity. *PLoS Pathog.* **6**, e1000953.

Ospina-Villa, J.D., Zamorano-Carrillo, A., López-Camarillo, C., Castañon-Sánchez, C.A., Soto-Sánchez, J., Ramírez-Moreno, M.E., and Marchat, L.A. 2015. Amino acid residues Leu135 and Tyr236 are required for RNA binding activity of CFIm25 in *Entamoeba histolytica*. *Biochimie* **115**, 44–51.

Pezet-Valdez, M., Fernández-Retana, J., Ospina-Villa, J.D., Ramírez-Moreno, M.E., Orozco, E., Charcas-López, S., Soto-Sánchez, J., Mendoza-Hernández, G., López-Casamicha, M., López-Camarillo, C., *et al.* 2013. The 25 kDa subunit of cleavage factor I_m is a RNA-binding protein that interacts with the poly(A) polymerase in *Entamoeba histolytica*. *PLoS One* **8**, e67977.

Ralston, K.S. and Petri, W.A. Jr. 2011.Tissue destruction and invasion by *Entamoeba histolytica*. *Trends Parasitol.* **27**, 254–263.

Schneider, C.A., Rasband, W.S., and Eliceiri, K.W. 2012. NIH Image to ImageJ: 25 years of image analysis. *Nat. Methods* **9**, 671–675.

Sikorski, T.W., Ficarro, S.B., Holik, J., Kim, T., Rando, O.J., Marto, J.A., and Buratowski, S. 2011. Sub1 and RPA associate with RNA polymerase II at different stages of transcription. *Mol. Cell.* **44**, 397–409.

Solis, C.F., Santi-Rocca, J., Perdomo, D., Weber, C., and Guillén, N. 2009. Use of bacterially expressed dsRNA to down regulate *Entamoeba histolytica* gene expression. *PLoS One* **4**, e8424.

Takiff, H.E., Chen, S.M., and Court, D.L. 1989. Genetic analysis of the *rnc* operon of *Escherichia coli*. *J. Bacteriol.* **171**, 2581–2590.

Tourrière, H., Chebli, K., and Tazi, J. 2002. mRNA degradation machines in eukaryotic cells. *Biochimie* **84**, 821–837.

Vasudevan, S., Tong, Y., and Steitz, J.A. 2007. Switching from repression to activation: microRNAs can up-regulate translation. *Science* **318**, 1931–1934.

Vinayagam, A., Stelzl, U., Foulle, R., Plassmann, S., Zenkner, M., Timm, J., Assmus, H.E., Andrade-Navarro, M.A., and Wanker, E.E. 2011. A directed protein Interaction network for investigating intracellular signal transduction. *Science Signaling.* **4**, rs8.

Wang, S.W., Asakawa, K., Win, T.Z., Toda, T., and Norbury, C.J. 2005. Inactivation of the pre-mRNA cleavage and polyadenylation factor Pfs2 in fission yeast causes lethal cell cycle defects. *Mol. Cell. Biol.* **25**, 2288–2296.

Yang, Q., Coseno, M., Gilmartin, G.M., and Doublié, S. 2011. Crystal structure of a human cleavage factor CFI_m25/CFI_m68/RNA complex provides an insight into poly(A) site recognition and RNA looping. *Structure* **19**, 368–377.

Zamorano, A., López-Camarillo, C., Orozco, E., Weber, C., Guillén, N., and Marchat, L.A. 2008. *In silico* analysis of EST and genomic sequences allowed the prediction of *cis*-regulatory elements for *Entamoeba histolytica* mRNA polyadenylation. *Comput. Biol. Chem.* **32**, 256–263.

Zhang, W., Wagner, B.J., Ehrenman, K., Schaefer, A.W., DeMaria, C.T., Crater, D., DeHaven, K., Long, L., and Brewer, G. 1993. Purification, characterization, and cDNA cloning of an AU-rich element RNA-binding protein, AUF1. *Mol. Cell. Biol.* **13**, 7652–7665.